27th ABCM International Congress of Mechanical Engineering
December 04-08, 2023, Florianópolis-SC, Brazil

COB-2023-0626
INVESTIGATION OF AN IDENTICAL METASTRUCTURE FOR VIBRATION ATTENUATION IN A CRANKSHAFT WITH NON-CONSTANT INERTIA

Nícolas da Silva Dias
Aline Souza de Paula
Universidade de Brasília, Campus Universitário Darcy Ribeiro, Faculdade de Tecnologia, Asa Norte, CEP 70.910-900, Brasília-DF

nicolassd29@gmail.com
alinedepaula@unb.br

Abstract. *Torsional vibrations are inherent in the operation of reciprocating machines, which is one of the leading causes of mechanical failures. This work analyzes the torsional vibration attenuation of a crankshaft of a single-cylinder reciprocating compressor when identical resonators are attached. The shaft is modeled by a continuous nonlinear system, considering the inertia variation of the crank-slider mechanism with rotation and under a concentrated harmonic excitation. Two main configurations are presented, without and with resonators. At first, the nonlinear and linearized systems are compared for two different crank length values. Results show that the systems present similar behaviors for a low value of the crank length. On the other hand, when the crank lengths are raised, the resonance frequencies are slightly shifted backward and the response exhibits nonlinear effects. The second case presents the system response when the resonators are attached. The performance of the resonators is evaluated for two crank length values as in the previous analysis. In both cases, the resonators can reduce the vibration amplitudes in the neighborhood of the target frequency, even when the nonlinearity is increased in the system response.*

Keywords: *torsional vibration, vibration attenuation, identical resonators, non-constant inertia.*

1. INTRODUCTION

Vibrations are an intrinsic phenomenon in rotating machines (Chandrashekar *et al.*, 2018). Typically, these vibrations manifest during startup, continuous operation, or shutdown (Wachel and Szenasi, 1993), being the leading causes of coupling failures, broken shafts, and worn gears, among others (Corbo and Melanoski, 1996). They are caused by the excessive forces and moments that vary cyclically with the periodicity given by the rotational speed of the system (Wachel and Tison, 1994). In this context, vibration control is one important subject, and it is studied extensively by the scientific community to ensure a long service life of these mechanical equipment.

Over the years, several researchers have proposed dynamic models for a better understanding of the bending and torsional vibrations in rotating systems. In the case of machines with crankshafts, such as internal combustion engines and reciprocating compressors, the torsional vibration analysis is more relevant. This is because the rotation of the shaft initiates the compression inside the cylinder performed by the crank sliding mechanism, which undergoes a periodic reciprocating motion resulting in vibration and noise (Liu *et al.*, 2019).

The first available studies in the literature consider discrete linear models with lumped parameters (Li *et al.*, 2022). However, as they are simplified, they often cannot adequately describe the system dynamics. It is common to assume that the crank-slider mechanism has constant inertia, but this approximation can lead to significant errors (Pasricha and Carnegie, 1979). The variable inertia of the mechanism enhances the realism in representing dynamic phenomena, as stated by the authors Pasricha and Carnegie (1976, 1979), Brusa *et al.* (1997), Metallidis and Natsiavas (2003), Huang *et al.* (2012), and results in nonlinear equations of motion. This nonlinearity gives rise to the emergence of a second resonance caused by the coupling of natural modes of the system (Draminsky, 1965; Hesterman and Stone, 1994, 1995).

In general, dynamical systems can be described by discrete or continuous models. The continuous modeling of the torsional vibration of crankshafts can be achieved by considering a uniform shaft, as defined by the classical problem (Inman, 2007), or non-uniform, assuming the variation of torsional stiffness along its length (Li, 2003; Wu, 2007). The crank-slider mechanism can be modeled as concentrated inertia elements introduced into the problem by boundary conditions (Qiao *et al.*, 2002) or directly in the governing equation (Gürgöze, 1984; Wu and Lin, 1990; Peng and Yan, 2022). Nevertheless, there is a lack of research covering the nonlinear model with variable inertia. Typically, the system is linearized to simplify the dynamic analysis (Koser and Pasin, 1995, 1997).

This work presents an analysis of vibration attenuation of the torsional vibration of a single-cylinder reciprocating compressor's crankshaft using metamaterials, showing the effects of the nonlinearity of inertia of the crank sliding mechanism. This paper is structured as follows. The next section describes the equations of motion of the crankshaft with the attached concentrated inertia, and its analytical solution uses the modal expansion theory. Two configurations are presented: without and with identical resonators. Then, numerical results are presented and discussed, showing the system response under a concentrated harmonic excitation for two cases. In the first case, the crankshaft response shows the effects of the non-constant inertia. On the other hand, the resonators attached produce a vibration attenuation located in a specific frequency range. Finally, the conclusions section summarizes the main achievements of this work.

2. CRANKSHAFT MODEL AND RESPONSE USING MODAL COORDINATES

The discrete system proposed by Metallidis and Natsiavas (2003) divides reciprocating machines into two components, the first represents the compressor itself, and the second is the load. In this context, the authors make sense of the use of load in the representation of the model, because it is about an internal combustion engine. However, herein this term is adapted for compressor systems. This work considers two concentrated inertia, one representing the crank-slider mechanism inertia of the compressor that varies with rotation, $I_e(\theta)$, and one constant representing the load, I_l. These two elements are connected to a shaft represented by a continuous system. Two external torques are considered, the cylinder resistive torque is described by T_c, and the electric motor torque is T_m, as is shown in Fig. 1a. The compressor inertia is determined by using the equivalent crank-slider mechanism inertia, which is represented by Fig. 1b.

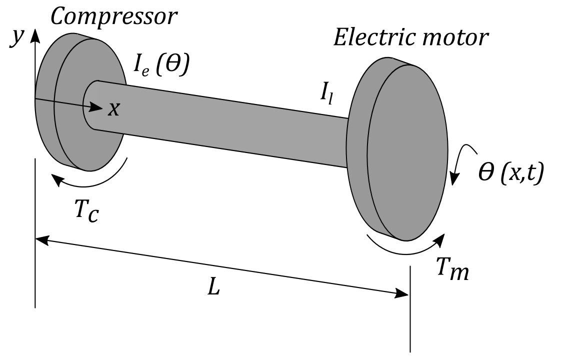

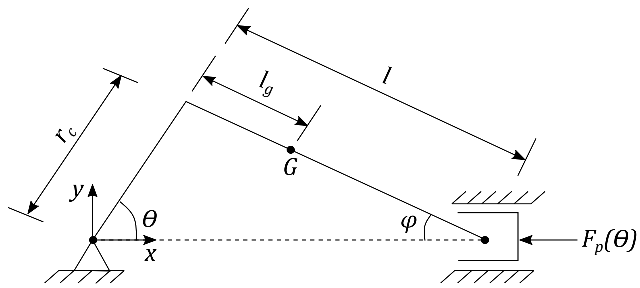

Figure 1: Model of a single-cylinder reciprocating compressor: (a) simplified model and (b) crank-slider mechanism.

2.1 Mathematical model

The crankshaft has a diameter d, Young's modulus of E, Poisson's ratio ν, shear's modulus $G = E/2(1+\nu)$, cross-section polar moment of inertia $J = \pi d^4/32$ and density ρ. The equation of motion is based on the problem of torsional vibration of an undamped shaft with a uniform cross-section and constant torsional stiffness GJ. The lumped inertia $I_e(\theta)$ is introduced into the equation together with the excitation torques T_m and T_c as follows:

$$\rho J \frac{\partial^2\theta(x,t)}{\partial t^2} + I_e(\theta)\delta(x-x_c)\frac{\partial^2\theta(x,t)}{\partial t^2} - GJ\frac{\partial^2\theta(x,t)}{\partial x^2} = T_m\delta(x-x_m) + T_c\delta(x-x_c), \tag{1}$$

the constant inertia I_l and I_0 are attached on the shaft extremities according to the boundary conditions (Inman, 2007):

$$GJ\frac{\partial\theta(0,t)}{\partial x} = I_0\frac{\partial^2\theta(0,t)}{\partial t^2}, \qquad GJ\frac{\partial\theta(L,t)}{\partial x} = -I_l\frac{\partial^2\theta(L,t)}{\partial t^2}. \tag{2}$$

The variable cylinder inertia and I_0, which it is the linearized form of $I_e(\theta)$ are obtained by Metallidis and Natsiavas (2003):

$$I_e(\theta) = I_c + m_1 r_c^2 + I_2\kappa^2(\theta) + (m_2+m_p)r_c^2\sin^2(\theta)[1+\kappa(\theta)]^2, \tag{3}$$

$$I_0 = I_c + m_1 r_c^2 + \frac{1}{2}(m_2+m_p)r_c^2, \tag{4}$$

being the parameters m_1, m_2, κ and λ defined by the following expressions:

$$m_1 = \left(1 - \frac{l_g}{l}\right) m_r, \qquad m_2 = \frac{l_g}{l} m_r, \qquad I_2 = I_g - m_1 l_g^2 - m_2 (l - l_g)^2, \tag{5}$$

$$\kappa(\theta) = \frac{\lambda \cos(\theta)}{\sqrt{1 - \lambda^2 \sin^2(\theta)}} \qquad \text{and} \qquad \lambda = \frac{r_c}{l}, \tag{6}$$

where I_2 is the additional inertia from a simplified double-mass system, I_c is the moment of inertia of the crank, I_g is the moment of inertia of the connecting rod center of mass, m_1 is the mass of the big end, m_2 is the mass of the small end, m_p is the piston mass, m_r is the mass of the connecting rod, l is the total length of the connecting rod, l_g is the length of the connecting rod center of mass, r_c is the crank length, $\delta(x)$ is the Dirac delta function, x_c is the cylinder position, x_l is the load position, and x_m is the electric motor position.

The variable inertia $I_e(\theta)$ can be expressed as the sum of two terms:

$$I_e(\theta) = I_0 + I_{nl}(\theta), \tag{7}$$

where $I_{nl}(\theta)$ corresponds to the nonlinear part.

Since the influence of I_0 was already incorporated for determining the mode shapes and natural frequencies of the crankshaft, only the nonlinear part of the non-constant inertia $I_e(\theta)$ must be considered in the equation of motion to evaluate the system response, as follows:

$$\rho J \frac{\partial^2 \theta(x,t)}{\partial t^2} + I_{nl}(\theta)\delta(x - x_c)\frac{\partial^2 \theta(x,t)}{\partial t^2} - GJ\frac{\partial^2 \theta(x,t)}{\partial x^2} = T_m \delta(x - x_m) + T_c \delta(x - x_c). \tag{8}$$

2.2 Solution using modal expansion

The crankshaft response is determined employing a modal expansion theory as addressed by Meirovitch (1997). Despite the nonlinear nature of the system under investigation, the dynamical response is assessed using modal expansion, assuming no nonlinear modal interactions, as suggested by Xia *et al.* (2020). The torsional displacement of the shaft is:

$$\theta(x,t) = \sum_{r=1}^{N} \eta_r(t)\phi_r(x), \tag{9}$$

where $\eta_r(t)$ is the modal coordinate of the r-th mode, $\phi_r(x)$ is r-th mode shape of the shaft with the concentrated inertia at the boundaries I_l and I_0, N is the total number of modes considered in the modal expansion. The modes shapes are inertia-normalized by Eq. 15 yields in:

$$\phi_r(x) = A_2 \left(cos\left(\frac{\beta_r x}{L}\right) - \frac{\beta_r I_0}{\rho J L} sin\left(\frac{\beta_r x}{L}\right)\right), \qquad r = 1, 2, 3, \ldots N, \tag{10}$$

with

$$A_2 = \sqrt{\frac{2}{\rho J L\left(1 + \left(\frac{\beta_r I_0}{\rho J L}\right)^2\right)}}, \tag{11}$$

where β_r is the r-th positive and real solution of the characteristic equation given by:

$$tg(\beta L) = \frac{\rho J L (I_0 + I_l)\beta L}{I_0 I_l (\beta L)^2 - \rho^2 J^2 L^2}. \tag{12}$$

Introducing the Eq. 9 in Eq. 8, assuming that the system is under a concentrated harmonic excitation $f(x,t) = F\delta(x - x_e)e^{i\omega t}$ located in the excitation position x_e , one obtains:

$$\sum_{r=1}^{N}\rho J\ddot{\eta}_r(t)\phi_r(x)+\sum_{r=1}^{N}I_{nl}(\theta)\delta(x-x_c)\ddot{\eta}_r(t)\phi_r(x)-\sum_{r=1}^{N}GJ\eta_r(t)\phi_r''(x)=F\delta(x-x_e)e^{i\omega t}. \tag{13}$$

Multiplying the Eq. 13 by $\phi_s(x)$ and integrating over the domain from $x = 0$ to $x = L$, results in:

$$\sum_{r=1}^{N}\int_0^L\rho J\ddot{\eta}_r(t)\phi_r(x)\phi_s(x)dx+\sum_{r=1}^{N}\int_0^L I_{nl}(\theta)\delta(x-x_c)\ddot{\eta}_r(t)\phi_r(x)\phi_s(x)dx-\sum_{r=1}^{N}\int_0^L GJ\eta_r(t)\phi_r''(x)\phi_s(x)dx$$
$$=\int_0^L F\phi_s(x)\delta(x-x_e)e^{i\omega t}dx. \tag{14}$$

The orthonormal conditions are described below:

$$\int_0^L\rho J\phi_r(x)\phi_s(x)dx=\delta_{rs}, \qquad r,s=1,2,\ldots \tag{15}$$

$$\int_0^L GJ\phi_r''(x)\phi_s(x)dx=-\omega_s^2\delta_{rs}, \qquad r,s=1,2,\ldots \tag{16}$$

where ω_s is the natural frequency of the r-th mode of the shaft with concentrated inertia at the boundaries I_l and I_0, and $()'$ denotes the derivative with respect to the space variable x.

Applying the orthonormal conditions represented by Eqs.15 and 16 one obtains the uncouple undamped equations of motion in modal coordinates:

$$\ddot{\eta}_s(t)+I_{nl}(\theta_{x_c})\phi_s^2(x_c)\ddot{\eta}_s(t)+\omega_s^2\eta_s(t)=F\phi_s(x_e)e^{i\omega t}, \qquad s=1,2,\ldots,N. \tag{17}$$

where $\theta_{x_c}=\theta(x_c,t)$, F is the amplitude and ω is the excitation frequency.

3. CRANKSHAFT WITH IDENTICAL RESONATORS

This section describes the formulation when resonators are attached to the crankshaft employing the modal expansion theory. The attachments are identical and tuned at the same frequency, to reduce the vibration amplitude in a specific frequency range. Figure 2 shows the crankshaft with evenly distributed identical resonators.

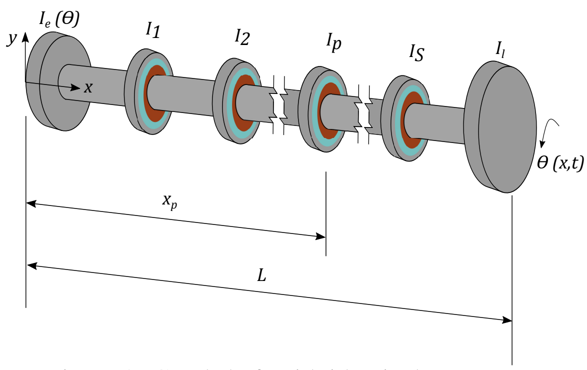

Figure 2: Crankshaft with identical resonators.

According to the work proposed by Sugino *et al.* (2017), the equation of motion of the crankshaft with evenly distributed identical resonators attached is represented by:

$$\rho J\frac{\partial^2\theta(x,t)}{\partial t^2}+I_{nl}(\theta)\delta(x-x_c)\frac{\partial^2\theta(x,t)}{\partial t^2}-GJ\frac{\partial^2\theta(x,t)}{\partial x^2}-\sum_{p=1}^{S}k_p\theta_p(t)\delta(x-x_p)=f(x,t), \tag{18}$$

and each resonator has the following equation of motion given as:

$$I_p\ddot{\theta}_p(t) + k_p\theta_p(t) + I_p\ddot{\theta}(x_p,t) = 0, \qquad p = 1,2,3,\dots,S \tag{19}$$

where k_p is the torsional stiffness of the $p-$th resonator, I_p is the inertia of the $p-$th resonator, $\theta_p(t)$ is the torsional relative displacement of the $p-$th resonator, x_p is the position of the $p-$th resonator, S is the total number of resonators and $f(x,t)$ is the external torque density.

Assuming that the crankshaft is subjected to a concentrated harmonic excitation as $f(x,t) = F\delta(x-x_e)e^{i\omega t}$ in the excitation position x_e. Using the modal expansion theory with N modes as $\theta(x,t) = \sum_{r=1}^{N}\eta_r(t)\phi_r(x)$ neglecting the nonlinear modal interactions, and employing the orthonormalization conditions defined in Eqs. 15, 16, results in the set of $N+S$ coupled equation of motions:

$$\ddot{\eta}_s(t) + I_{nl}(\theta_{x_c})\phi_s^2(x_c)\ddot{\eta}_s(t) + \omega_s^2\eta_s(t) - \sum_{p=1}^{S}k_p\theta_p(t)\phi_s(x_p) = F\phi_s(x_e)e^{i\omega t}, \qquad s = 1,2,3,\dots,N \tag{20}$$

$$\ddot{\theta}_p(t) + \omega_p^2\theta_p(t) + \sum_{s=2}^{N}\ddot{\eta}_s(t)\phi_s(x_p) = 0, \qquad p = 1,2,3,\dots,S \tag{21}$$

where ω_p is the natural frequency of the $p-$th resonator, being equal for all of them.

4. FREQUENCY DOMAIN SWEEP

This section presents a numerical procedure for determining the response of a dynamical system in the frequency domain, as there is no closed-form expression for the frequency response function (FRF) in the case of nonlinear systems. The FRF is obtained by calculating the FFT (Fast Fourier Transform) from a temporal response of a harmonic excitation sweep. The crankshaft is subject to a harmonic excitation with frequency ω, which is considered a range of frequency. From the uncouple equations in modal coordinates (Eq. 17), introducing modal damping ξ_s, one obtains:

$$\ddot{\eta}_s(t) + I_{nl}(\theta_{x_c})\phi_s^2(x_c)\ddot{\eta}_s(t) + 2\xi_s\omega_s\dot{\eta}_s(t) + \omega_s^2\eta_s(t) = F\phi_s(x_e)e^{i\omega t}, \qquad s = 1,2,3,\dots,N \tag{22}$$

where the excitation frequency ω varied linearly over time as described by

$$\omega = \frac{\omega_f - \omega_0}{2}t + \omega_0 \tag{23}$$

where ω_0 is the initial frequency and ω_f is the final excitation frequency.

The modal coordinates $\eta_s(t)$ and the harmonic excitation $f(x,t)$ are obtained from the employed fourth-order Runge-Kutta numerical method in the state equations:

$$\{s_e\} = \begin{Bmatrix}\eta_s(t)\\ \dot{\eta}_s(t)\end{Bmatrix}, \qquad \{\dot{s}_e\} = \begin{Bmatrix}\dot{\eta}_s(t)\\ \ddot{\eta}_s(t)\end{Bmatrix} = \begin{Bmatrix}\dot{\eta}_s(t)\\ \frac{F\phi_s(x_e)e^{i\omega t} - 2\xi_s\omega_s\dot{\eta}_s(t) - \omega_s^2\eta_s(t)}{1 + I_{nl}(\theta_{x_c})\phi_s^2(x_c)}\end{Bmatrix},$$
$$\text{with} \qquad s = 1,2,3,\dots,N. \tag{24}$$

Therefore, the FRF can be determined in the response position x_r using the FFT from the following relation:

$$\alpha_{re}(\omega) = \frac{FFT[\theta(x_r,t)]}{FFT[f(x_e,t)]} = \frac{FFT\left[\sum_{s=1}^{N}\eta_s(t)\phi_s(x_r)\right]}{FFT[F\phi_s(x_e)e^{i\omega t}]}. \tag{25}$$

This approach follows the same path when identical resonators are attached to the crankshaft.

5. RESULTS AND DISCUSSION

This section shows the steady-state responses in the frequency domain when the crankshaft is subject to harmonic excitation, as well as evaluating the vibration reduction produced by the identical resonators. Two main configurations are presented, in the first without resonators, the nonlinear model is compared with the linearized one. In the second case, the resonators are attached to the system to attenuate torsional vibrations in a specific frequency range. The simulations are carried out for different values of the non-constant inertia $I_{nl}(\theta_{x_c})$, to explore the nonlinear effects in the crankshaft response when the nonlinearity is increased. Table 1 presents the system's parameters used in the numerical investigations, which are based on the works of Huang *et al.* (2012) and Metallidis and Natsiavas (2003).

Table 1: System parameters.

Inertia of the crank, I_c	0.01783 kg.m^2
Inertia of the connecting rod center of mass, I_g	0.0458 kg.m^2
Mass of the connecting rod, m_r	3.8 kg
Mass of the piston, m_p	4.026 kg
l_g/l	0.29
Crank length, r_c	0.0725 m
Length of the shaft, L	1 m
Diameter of the shaft, d	0.06 m
Young's modulus of the shaft, E	221 GPa
Density of the shaft, ρ	7800 kg/m^3
Poisson's ratio of the shaft, ν	0.3
Inertia of the load, I_l	0.165 kg.m^2
Connecting rod length, l	0.262 m
Modal damping of the shaft, ξ_s	0.002
Harmonic excitation amplitude, F	1×10^8 N.m
Initial harmonic excitation frequency, ω_0	1 Hz
Final harmonic excitation frequency, ω_f	18000 Hz
Number of modes in modal expansion, N	10
Number of attached resonators, S	10

In the first case, the dynamic analysis compares the nonlinear and linear systems under harmonic excitation without resonators. The equations of motion (Eqs. 24) are numerically integrated employing the fourth-order Runge-Kutta method, with the incremental step $h = 6.283 \times 10^{-7}$ s and the initial conditions $\eta_2(0) = \eta_3(0) = \cdots = \eta_{10}(0) = 0$ rad/m, $\dot{\eta}_1(0) = \dot{\eta}_2(0) = \cdots = \dot{\eta}_{10}(0) = 0$ rad/m.s. It is worth mentioning that the simulations consider only non-zero natural frequencies.

Figure 3 shows system responses for two crank length values. The continuous blue line represents the response of the linearized system (L), while the dashed orange line is the nonlinear (NL) system behavior. For lower crank length, $r_c = 72.5$ mm, we observe that resonance frequencies match when compared to the linear one, even though some antiresonance peaks are shifted (Fig. 3a). However, when the crank length is raised to $r_c = 200$ mm (Fig. 3b), the resonance frequencies have shifted slightly backward due to the increase of the nonlinearities.

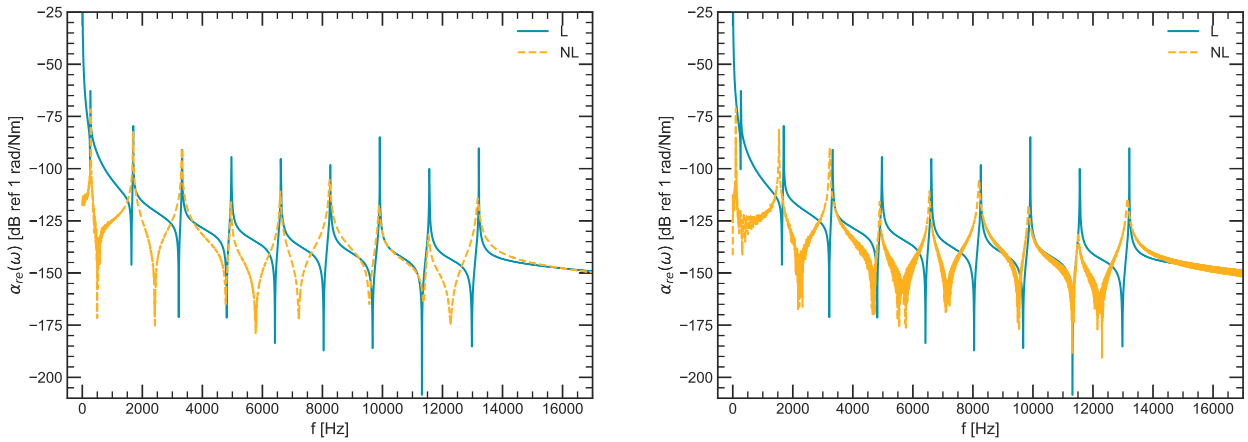

(a) $r_c = 72.5$ mm (b) $r_c = 200$ mm

Figure 3: FRFs of linear (L) and nonlinear (NL) systems for different crank lengths r_c.

The second case presents the configuration when identical resonators are attached to the system. Figure 4 shows system responses without resonators represented by the continuous blue line and with attached resonators described by the dashed orange line. The shaded region is the estimated linear local bandgap for finite and continuous metastructures expressed by Sugino *et al.* (2017) as:

$$\omega_t < \omega < \omega_t\sqrt{1+\mu}, \tag{26}$$

where ω_t is the target frequency of the resonators and μ is the inertia ratio of the total inertia of the resonators to the total inertia of the crankshaft as follows:

$$\mu = \frac{\sum_{p=1}^{S} I_p}{\rho JL + I_0 + I_l} = \frac{I_p S}{\rho JL + I_0 + I_l}. \tag{27}$$

The numerical investigations assume that the inertia ratio $\mu = 0.3$ and the resonators are tuned in $\omega_t = 4967.154$ Hz, which corresponds to the fifth resonance peak. As in the previous case, the performance of the resonators is analyzed for two crank length values. In both cases, for a low and high value of the crank length $r_c = 72.5$ mm (Fig. 4a) and $r_c = 200$ mm (Fig. 4b), respectively, the metastructure attenuates the torsional vibrations producing a bandgap with bandwidth according to Eq. 26, even when the nonlinearities are increased.

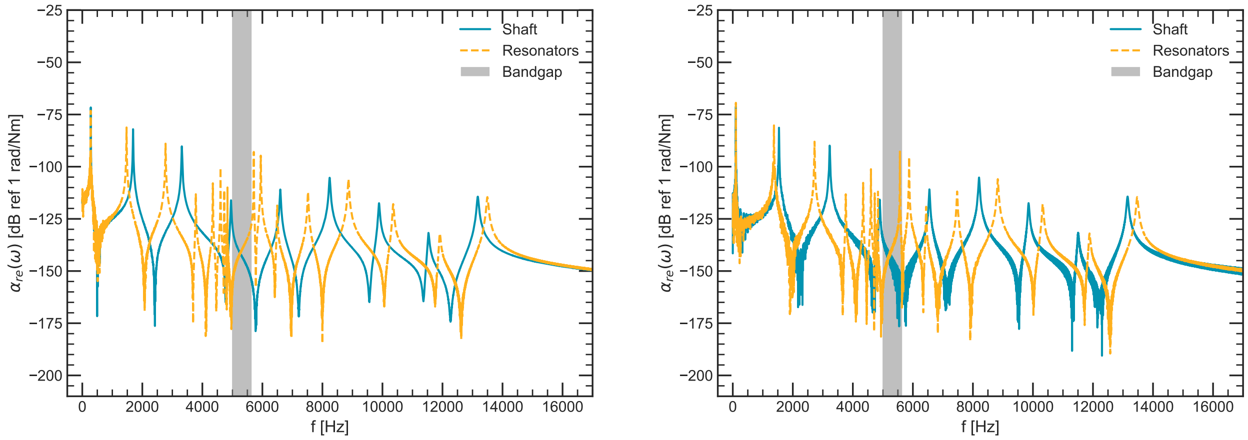

(a) $r_c = 72.5$ mm (b) $r_c = 200$ mm

Figure 4: FRFs of the nonlinear system with identical resonators for different crank lengths r_c.

The used procedure to obtain the FRF of the nonlinear system is an alternative for a preliminary analysis with low computational cost. However, it does not capture the richness of details of the dynamic behavior. This approach was employed as an initial assessment to identify situations where nonlinearities play a significant role. In these situations, it is necessary to evaluate the response in more detail using other suitable tools that can identify various aspects, such as the type of system response, the occurrence of dynamical jumps, and other relevant aspects.

6. CONCLUSIONS

This work investigates the torsional vibration attenuation in a crankshaft of a reciprocating compressor with a single-cylinder using identical resonators. The shaft is modeled by a continuous nonlinear system, considering the inertia variation of the crank-slider mechanism with the rotation $I_e(\theta)$, and subjected to a concentrated harmonic excitation. Two main configurations were considered, without and with the attached resonators. In the first case, the responses of the nonlinear and the linearized systems are compared considering two different crank length values r_c. The results show that for a low value of the crank length, the resonance frequencies match while the antiresonance peaks are shifted when compared to the linearized case. On the other hand, when the crank length is increased, the resonance frequencies are slightly moved backward and the nonlinear effects are evident in the response. In the second case, the performance of the resonators attached to the crankshaft is evaluated for two crank length values as in the previous analysis. Results showed that the resonators successfully reduced the vibration amplitudes in the region near the target frequency, even when the nonlinearity is raised in the system response.

7. ACKNOWLEDGEMENTS

The authors are grateful to the Brazilian National Council of Research (CNPq - Brazil) to CAPES and FAPDF, process 00193-00001139/2021-57, for their support.

8. REFERENCES

Brusa, E., Delprete, C. and Genta, G., 1997. “Torsional vibration of crankshafts: Effects of non-constant moments of inertia”. *Journal of Sound and Vibration*, Vol. 205, No. 2, pp. 135–150.

Chandrashekar, G., Raj, W., Godwin, C. and Paul, P.S., 2018. “Study on the influence of shaft material on vibration in rotating machinery”. *Materials Today: Proceedings*, Vol. 5, No. 5, pp. 12071–12076.

Corbo, M.A. and Melanoski, S.B., 1996. “Practical design against torsional vibration.” In *Proceedings of the 25th Turbomachinery Symposium*. Texas A&M University, Turbomachinery Laboratories, Dallas, pp. 189–222.

Draminsky, P., 1965. “An introduction to secondary resonance”. *Shipbuilding and Marine Engineering International*, Vol. 88, pp. 22–26.

Gürgöze, M., 1984. “A note on the vibrations of restrained beams and rods with point masses”. *Journal of Sound and Vibration*, Vol. 96, No. 4, pp. 461–468.

Hesterman, D. and Stone, B., 1994. “A systems approach to the torsional vibration of multi-cylinder reciprocating engines and pumps”. *Proceedings of the Institution of Mechanical Engineers, Part C: Journal of Mechanical Engineering Science*, Vol. 208, No. 6, pp. 395–408.

Hesterman, D. and Stone, B., 1995. “Secondary inertia effects in the torsional vibration of reciprocating engines—a literature review”. *Proceedings of the Institution of Mechanical Engineers, Part C: Journal of Mechanical Engineering Science*, Vol. 209, No. 1, pp. 11–15.

Huang, Y., Yang, S., Zhang, F., Zhao, C., Ling, Q. and Wang, H., 2012. “Non-linear torsional vibration characteristics of an internal combustion engine crankshaft assembly”. *Chinese Journal of Mechanical Engineering (English Edition)*, Vol. 25, No. 4, pp. 797–808.

Inman, D.J., 2007. *Engineering vibration*. Pearson Education, New Jersey, 3rd edition.

Koser, K. and Pasin, F., 1995. “Continuous modelling of the torsional vibrations of the drive shaft of mechanisms”. *Journal of Sound and Vibration*, Vol. 188, No. 1, pp. 17–24.

Koser, K. and Pasin, F., 1997. “Torsional vibrations of the drive shafts of mechanisms”. *Journal of Sound and Vibration*, Vol. 199, No. 4, pp. 559–565.

Li, Q., 2003. “Torsional vibration of multi-step non-uniform rods with various concentrated elements”. *Journal of Sound and Vibration*, Vol. 260, No. 4, pp. 637–651.

Li, T., Chen, Z., Zhang, K., Wang, J. and Huang, Z., 2022. “Analysis of the influence of piston–cylinder friction on the torsional vibration characteristics of compressor crankshaft system”. *Nonlinear Dynamics*, Vol. 110, No. 2, pp. 1323–1338.

Liu, S., Li, W., Shuai, Z. and Chen, M., 2019. “Vibration analysis of a single-cylinder reciprocating compressor considering the coupling effects of torsional vibration”. *Shock and Vibration*, Vol. 2019.

Meirovitch, L., 1997. *Principles and techniques of vibrations*, Vol. 1. Prentice Hall, New Jersey.

Metallidis, P. and Natsiavas, S., 2003. “Linear and nonlinear dynamics of reciprocating engines”. *International Journal of Non-Linear Mechanics*, Vol. 38, No. 5, pp. 723–738.

Pasricha, M.S. and Carnegie, W.D., 1979. “Formulation of the equations of dynamic motion including the effects of variable inertia on the torsional vibrations in reciprocating engines, part i”. *Journal of Sound and Vibration*, Vol. 66, No. 2, pp. 181–186.

Pasricha, M. and Carnegie, W., 1976. “Effects of variable inertia on the damped torsional vibrations of diesel engine systems”. *Journal of Sound and Vibration*, Vol. 46, No. 3, pp. 339–345.

Peng, T. and Yan, Q., 2022. “Torsional vibration analysis of shaft with multi inertias”. *Scientific Reports*, Vol. 12.

Qiao, H., Li, Q. and Li, G., 2002. “Torsional vibration of non-uniform shafts carrying an arbitrary number of rigid disks”. *J. Vib. Acoust.*, Vol. 124, No. 4, pp. 656–659.

Sugino, C., Xia, Y., Leadenham, S., Ruzzene, M. and Erturk, A., 2017. “A general theory for bandgap estimation in locally resonant metastructures”. *Journal of Sound and Vibration*, Vol. 406, pp. 104–123.

Wachel, J.C. and Szenasi, F.R., 1993. “Analysis of torsional vibrations in rotating machinery”. In *Proceedings of the 22nd Turbomachinery Symposium*. Texas A&M University. Turbomachinery Laboratories, Dallas, pp. 127–151.

Wachel, J. and Tison, J., 1994. “Vibrations in reciprocating machinery and piping systems”. In *Proceedings of the 23rd Turbomachinery Symposium*. Texas A&M University. Turbomachinery Laboratories, Dallas, pp. 243–272.

Wu, J.S. and Lin, T.L., 1990. “Free vibration analysis of a uniform cantilever beam with point masses by an analytical-and-numerical-combined method”. *Journal of Sound and Vibration*, Vol. 136, No. 2, pp. 201–213.

Wu, J.J., 2007. “Torsional vibration analyses of a damped shafting system using tapered shaft element”. *Journal of Sound and Vibration*, Vol. 306, No. 3-5, pp. 946–954.

Xia, Y., Ruzzene, M. and Erturk, A., 2020. “Bistable attachments for wideband nonlinear vibration attenuation in a metamaterial beam”. *Nonlinear Dynamics*, Vol. 102, pp. 1285–1296.

9. RESPONSIBILITY NOTICE

The authors are solely responsible for the printed material included in this paper.